Research Article

Received: 14 April 2018 Revised: 27 July 2018 Accepted article published: 22 August 2018 Published online in Wiley Online Library: 3 October 2018

(wileyonlinelibrary.com) DOI 10.1002/ps.5183

Spatial global assessment of the pest *Bagrada hilaris* (Burmeister) (Heteroptera: Pentatomidae): current and future scenarios

Mario A Carvajal,[a] Alberto J Alaniz,[a*] Ignacio Núñez-Hidalgo[a,b] and Carlos González-Césped[a,c]

Abstract

BACKGROUND: The insect *Bagrada hilaris* (Burmeister) an important pest worldwide, mainly due to the serious economic losses incurred and the large number of zones invaded. However, current and future spatial distributions of this pest, and the total area of cropland potentially affected have not been estimated. Here, we aim to: (1) estimate the potential geographic distribution of *B. hilaris*; (2) quantify the total area of cropland potentially affected worldwide, and in two recently colonized zones (California and Chile); and (3) estimate future changes in distribution under different climate change scenarios.

RESULTS: We found that *B. hilaris* shows high environmental suitability in Mediterranean and arid regions, potentially affecting 1 108 184.1 km^2 of cropland worldwide. The most affected continents were Asia and America, with 309 659.8 and 294 638.6 km^2 of cropland at risk. More than 50% of cropland areas are at risk in seven countries. In California and central Chile, 43.7% and 50% of susceptible crops are at a high level of risk, respectively. Climate change scenarios predict an increase in the potential distribution of *B. hilaris* worldwide; America being the most affected continent.

CONCLUSIONS: Our results provide a spatially explicit baseline from which to focus efforts on the prevention, management and control of this pest worldwide.

Supporting information may be found in the online version of this article.

Keywords: risk level; climate change; painted bug; biological invasion; pest ecological modelling; food security

1 INTRODUCTION

Biological invasions are one of the main problems for biosecurity worldwide, mainly due to their effects on biological assemblages in the colonized zones and their potential economic impacts.[1,2] In newly colonized zones, the invasive species experiences a series of phases after its introduction–establishment/naturalization, spread and impact.[3] Management during these phases involves very different economic and logistic efforts, focused on prevention, control, mitigation and eradication of the invasive species.[4] Currently, biological invasions and human settlements are closely related to economic development, one of the most important concerns in the 21st century.[5,6] Climate change can modulate the effects of biological invasions by changing species' phenology, increasing their activity, shifting their distribution, modifying their interaction networks in colonized zones and ultimately changing ecosystem processes.[5,7] Shifts in the distribution of pests could increase their potential colonizable area, expanding areas of affected cropland.[8] These shifts in distribution range may represent a threat to the management and control of pests, hence knowledge about the future potential distribution of these invasive species can contribute to management actions.[9] The arrival of pest organisms in new areas due to climate change could represent a threat to food security, particularly in zones where access to water for crop irrigation is difficult due to periods of severe drought.[10–12]

One of the most important recent pests is *Bagrada hilaris*, a bug native to eastern and southern Africa and Asia.[13] This invasive species has colonized numerous regions of the world, with serious effects on brassica crops.[13,14] The main negative effect of this insect is the damage it causes to plant leaves, reducing chlorophyll generation and leaf area mainly on newer leaf tissues of cotyledons and two-leaf plants.[15,16] The species is an important pest in the Old World, mainly India, Africa, Southern Europe, Middle East and Southeast Asia.[13] In the New World, arrival of this species is

* Correspondence to: AJ Alaniz, Centro Ecología Espacial y Medio Ambiente – Ecogeografía, Miguel Claro 2550, Nuñoa, Santiago, Chile. E-mail: alberto.alaniz@ug.uchile.cl

a Centro de Estudios en Ecología Espacial y Medio Ambiente – Ecogeografía, Miguel Claro 2550, Nuñoa, Santiago, Chile

b Laboratorio de Ecología Geográfica. Facultad de Ciencias, Universidad de Chile, Las Palmeras 3425, Ñuñoa, Santiago, Chile

c Laboratorio de Entomología, Facultad de Ciencias Naturales y Exactas, Universidad de Playa Ancha, Valparaíso, Chile. Av. Sta. Rosa 11735, La Pintana, Santiago, Chile

recent; it was accidentally introduced into California in 2008 and by 2014 had spread significantly across the West Coast of the USA.[13] In the USA and Mexico, *B. hilaris* has had serious effects on agriculture, with important economic losses (approximately US $1 billion in 2013 in California and more than US $679 million in Monterrey).[17–19] This insect was not present in South America until 2016, when it was accidentally introduced into central Chile, where it was reported for first time near the city of Santiago.[20] Since then, reports of *B. hilaris* in the Chile have increased in both number and spatial reach, two unambiguous indications that the insect is in the spreading stage of invasion.[21,22]

Current and future potential distributions of this pest have not been estimated, nor have the potentially affected croplands worldwide. Accordingly, the aims of this study are to: (1) estimate the current potential distribution of *B. hilaris*; (2) quantify potentially affected cropland areas by country, considering levels of potential risk at a global level and in two recently colonized zones (California and Chile); and (3) predict future potential distribution considering climate change scenarios on a global level.

2 METHODS

2.1 Estimation of the current potential distribution of *B. hilaris* worldwide

Ecological niche modeling based on the maximum entropy technique is the main approach used to estimate the potential distribution of this invasive species.[23] The ecological niche model (ENM) uses two main sets of input data; a series of environmental layers as niche predictor variables and a set of occurrences of the target species. We used as environmental layers the 19 bioclimatic layers, wind speed, water vapor pressure and solar radiation from the Worldclim v.2 project.[24] In addition, we included the human footprint layer from SEDAC-NASA[25] which is associated with anthropogenic influence and disturbance. All the environmental layers were at a pixel resolution of 1 km^2. A worldwide data set of occurrences was compiled from the Global Biodiversity Information Facility,[26] INaturalist (https://www.inaturalist.org/) and from published articles,[21,27–34] giving a total of 415 occurrences (Table S1).

To reduce the spatial autocorrelation of the occurrence data set, a spatial rarefy function was performed in a Geographic Information System (GIS). This process identified occurrence clusters, and then selected and removed the highly autocorrelated ones within clusters, maintaining random occurrences separated by >5 km.[35] We generated an exploratory ENM in MaxEnt v. 3.4.1[23] using all the environmental layers and the non-autocorrelated occurrences data set, calculating the percentage contribution and permutation importance for each variable. The normality of predictor environmental variables was tested with the Shapiro–Wilk test.[36] To reduce the over-fitting associated with co-linearity among predictor variables, a non-parametric multiple correlation matrix expressed in a correlogram was then generated by calculating the absolute correlation coefficients.[37] Finally, we selected the environmental variables with most relevance in the exploratory ENM and with correlation coefficients less than ± 0.7.

We projected the potential global niche, aiming to estimate zones of high suitability for the species associated with its ecological niche requirements.[38–41] This projection was performed by generating an ENM in MaxEnt with a five-fold cross-validation technique, using as input data the non-autocorrelated occurrences and only the selected predictor environmental variables. We used the Cloglog algorithm of MaxEnt, which estimates the potential abundance of an organism based on the suitability of the habitat for the target organism.[23] The accuracy of the model was assessed through the area under the receiver operator characteristic curve (AUC). We applied a random forest algorithm (RF) and partial least squares regression analysis (PLS) as *a posteriori* tests to measure the contribution of each variable to the final model. Finally, we analyzed the contribution of predictor variables and the response curves of environmental suitability for the species.

All statistical analyses and process were performed using R environment (R Development Core Team, 2008).

2.2 Quantification of the potential affected cropland areas

Potentially affected croplands were quantified using as input data the current ENM of *B. hilaris* and maps of global cropland extent. First, we considered the probabilities under the 10 percentile threshold (statistically non-significant probabilities) of training presence as non-significant,[39] excluding them from the risk analysis. We reclassified the statistically significant probabilities of the ENM in three equal intervals of probabilities: low, medium, and high. These levels were considered as a proxy for the expected risk produced on the croplands, based on the potential abundance of the organism modeled in MaxEnt.[23]

To quantify the potentially affected cropland we used the 'Global Food Security-support Analysis Data 30 meter (GFSAD30) Cropland Extent data product' from NASA. This map is a global cropland cover map for 2015 with a pixel resolution of 30 m, constructed using: (1) remote sensing images from MODIS, Landsat™ and other high-resolution sensors in some specific areas; (2) thematic maps of cropland extent and local agriculture censuses; (3) road networks; and (4) additional geospatial data including elevation, slope, aspect and ecological region. This product was generated thorough compilation of several published studies and it is the most up-to date and finest scale product currently available.[42–52] We used a nearest neighbor interpolation algorithm to resample the original resolution GFSAD30 cover (30 m^2) to 500 m^2, aiming to facilitate data processing at the world level. The resampled world map of croplands was then overlapped with the reclassified ENM of *B. hilaris* (potential abundance), to give a map of potentially affected croplands that corresponds to a spatially explicit estimation of the expected risk. This map represents areas of cropland potentially exposed to different abundance levels of *B. hilaris*. Finally, the results are expressed by continent and country, showing the total potentially affected area (in hectares) and the relative area of croplands affected by country (percentage of the total cropland area in the country) (Table S2).

In addition, we estimate the potentially affected crops (cruciferous and others) in two recently invaded zones: California (USA) and central Chile. For the California assessment, we used the satellite product 'USDA NASS Cropland Data Layers', which classified croplands into 131 types at a spatial resolution of 30 m for 2017.[53] Based on published studies about potential hosts plants, we selected 18 vulnerable cropland types that were reclassified as susceptible crops; this map was then overlapped with the *B. hilaris* expected risk map quantifying the areas per expected risk level.[54–56] For central Chile, we followed Zhao *et al.*[57] who mapped land cover types at 30 m of spatial resolution for 2014. This product identified five cropland types, one of which was associated with susceptible crops (cruciferous), despite including other crop types also. We then overlapped the susceptible crops with the *B. hilaris* expected risk map, quantifying the areas per expected risk level.

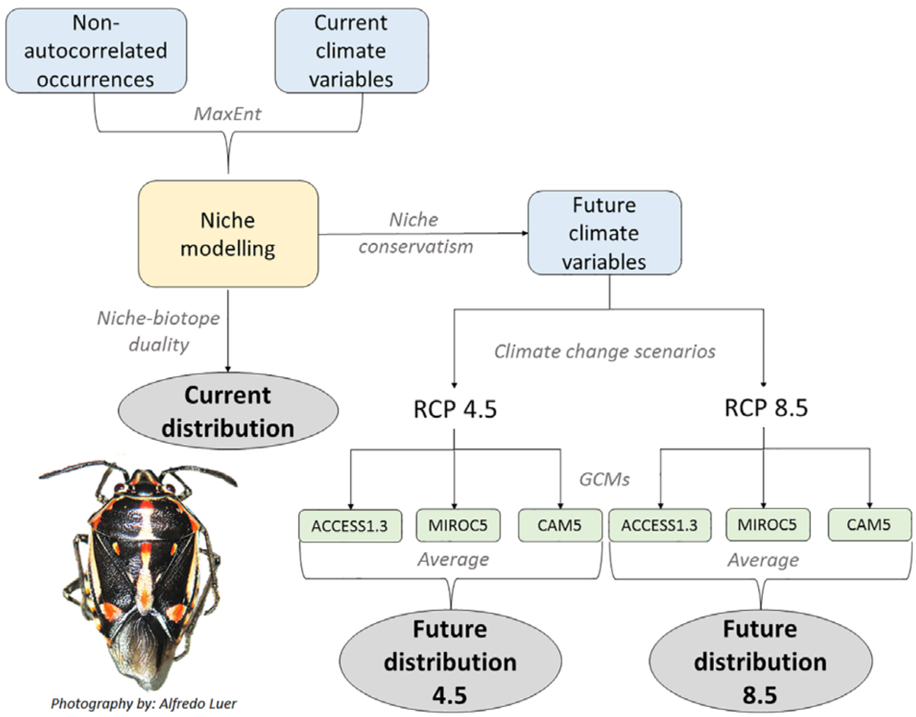

Figure 1. Diagram of the methodological approach.

2.3 Estimation of future potential distribution of *B. hilaris* worldwide

Estimation of the future distribution of organisms is based on niche conservatism theory, which proposes that species do not change their niche requirements in time and space.[38] This approach is based on modeling the species niche under current environmental conditions, allowing estimation of its spatial distribution. Once the niche is modeled it is projected into future environmental conditions, estimating its future spatial distribution.[58,59] To estimate the future potential distribution, we generated ENMs in MaxEnt 3.4.1,[23] using as input data the non-spatially autocorrelated occurrences, but changing the environmental variable data set. We included only bioclimatic variables, aiming to generate a projection based on climate because the other variables are not available for climate change scenarios (wind speed, water vapor pressure, solar radiation and human footprint). We also included elevation as a predictor variable because the niche projection in time and space achieves better performance considering topography.[60] According to this, to generate the ENM, we used the 19 bioclimatic variables in the current time (present) to model the species niche and its projection, considering climate change scenarios to estimate the future spatial distribution.

Future distribution of *B. hilaris* was estimated considering two climate change scenarios projected for 2050, Representative Concentration Pathway (RCP) 4.5 and RCP 8.5. These scenarios were proposed by the Intergovernmental Panel for Climate Change (IPCC) in their Fifth Assessment Report of Climate Change (AR5).[61] Each scenario represents the radiative force estimated for 2050 based on the predicted greenhouse gas emissions. We used an optimistic scenario (RCP 4.5) and a pessimistic scenario (RCP 8.5). We selected three general circulation models (GCMs), the Australian Community Climate and Earth System Simulator (ACCESS1.3),[62] Model for Interdisciplinary Research on Climate (MIROC5)[63] and Community Atmosphere Model (CAM5).[64] This GCM uses the IPCC RCP scenarios to estimate the future climate conditions in a spatially explicit way.

We first modeled the species niche with current climatic conditions. To do this, we generated an exploratory ENM using the current 19 bioclimatic variables plus altitude, calculating the percentage contribution and permutation importance of each variable in the prediction. We then generated a multiple correlation matrix expressed in a correlogram, calculating the Spearman rank correlation index.[37] We performed a final model using only the non-autocorrelated occurrence data set and the variables with the greatest contribution to the exploratory model with lower correlation values (less than ± 0.7). The model used the Cloglog algorithm and a five-fold cross-validation technique. Finally, we projected the modeled niche into future conditions represented by GCM for each RCP scenario (six projections, three per scenario) (Fig. 1).

In GIS software, we calculated the average suitability from the three GCMs, considering the two RCP scenarios for each GCM. We considered as significant suitability threshold values over the 10 percentile training presence. The accuracy of the projection was evaluated with Multivariate Environmental Similarity Surface (MESS) analysis, which allows estimation of the closeness of a given point to the distribution point, identifying the quality of the projection in a spatially explicit way. An average MESS analysis was generated by considering the MESS values of each replicate for each model (average MESS per niche model).[39] Finally, the accuracy of the model was evaluated through ROC analysis.

We analyzed the spatial changes between the current and future distribution ranges, quantifying the areas of contraction and expansion.

$$\text{Current} = \text{Contraction} + \text{No Change}$$
$$\text{Change} = (\text{Expansion} - \text{Contraction})/\text{Current}$$

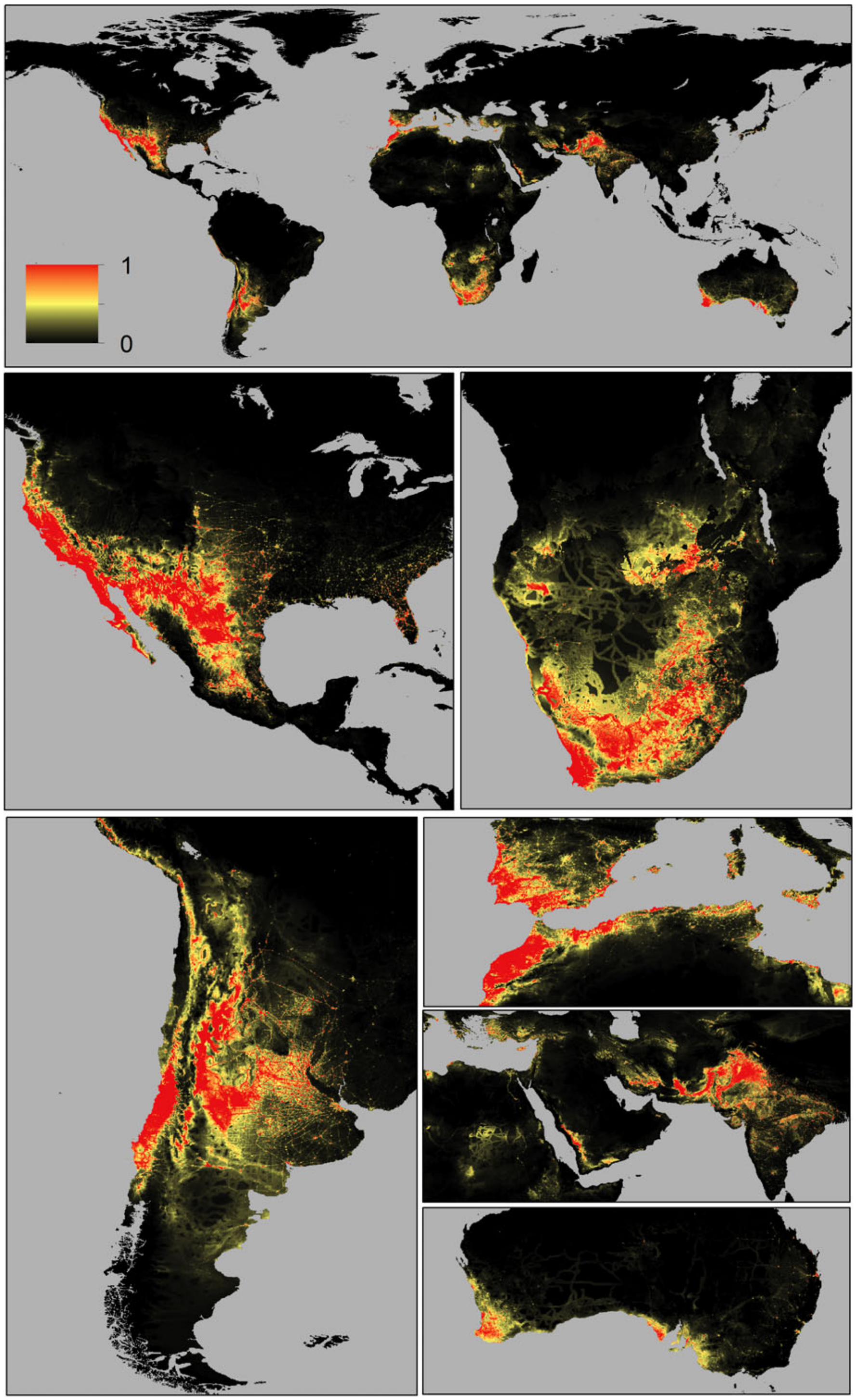

Figure 2. Current potential distribution of *Bagrada hilaris*. The level of environmental suitability appears as a color gradation from 0 (lower suitability, black) to 1 (higher suitability, red). (Upper) Global map of suitability. (Lower) Specific continents (downloadable as File S1).

3 RESULTS

3.1 Estimation of the current potential distribution of *B. hilaris* worldwide

The final ENM reached an AUC of 0.986 ± 0.005, predicting potential distribution in the five continents. The variable with the most significant contribution was the human footprint, at 48.7%, followed by isothermality and precipitation in the warmest quarter, at 19% and 17.4%, respectively. RF analysis showed an increase in the mean squared error (MSE) of 76.8% in the model when the human footprint variable was subtracted, highlighting the importance of this predictor (Fig. S1). This result was corroborated by PLS, confirming the human footprint as the most important predictor for the species (Fig. S2). The response curve for the human footprint showed a sigmoidal pattern, reaching a peak of suitability of $\sim$ 70% of the human footprint index. By contrast, isothermality showed a Gaussian pattern with a peak of suitability at 55%,

Table 1. Cropland areas potentially affected by *Bagrada hilaris* (× 10^3 km)

	Risk level			
Continent	High	Medium	Low	Total
Africa	51.4	63.8	86.8	202.0
Oceania	75.7	70.7	37.8	184.3
America	76.5	86.1	132.1	294.6
Asia	97.1	110.3	102.3	309.7
Europe	38.4	43.5	35.7	117.6
Total	339.0	374.4	394.7	1108.2

whereas the precipitation in the warmest quarter showed a peak at 0 mm precipitation, decreasing quickly with the increase in precipitation (Fig. S3).

There is suitability in all continents for *B. hilaris*, mainly in Mediterranean zones from ∼20° to 40° in the Northern Hemisphere and from 15° to 40° in the Southern Hemisphere. *B. hilaris* has high suitability in the West Coast of the USA and the central zone of Mexico, whereas in South America the main suitability is located mostly in central Chile and Argentina. In Europe, the greatest suitability is concentrated in Portugal, Spain, Italy (mainly in the Mediterranean Sea islands) and the coastal zone of Turkey. In Africa, the suitability is located mainly in the northern coast near the Strait of Gibraltar (Algeria and Morocco), and in the southern coast across the Cape of Good Hope (South Africa, Namibia, Zimbabwe and Zambia). In Oceania, the suitability is concentrated in the southern coasts of Australia, particularly near the cities of Perth and Adelaide. In Asia, the suitability occurs mainly in Pakistan, India and southern Iran (Fig. 2).

3.2 Quantification of the potentially affected cropland areas

Globally, 1 108 184.1 km^2 are at risk associated with *B. hilaris*. Of these areas, 35.6% have a high level of risk, 33.8% have a medium level and 30.6% have a low level (Table 1). Of the total surface of croplands potentially affected, 27.9% is in Asia, followed by America, Africa, Oceania and Europe with 26.6%, 18.2%, 16.6% and 10.6%, respectively.

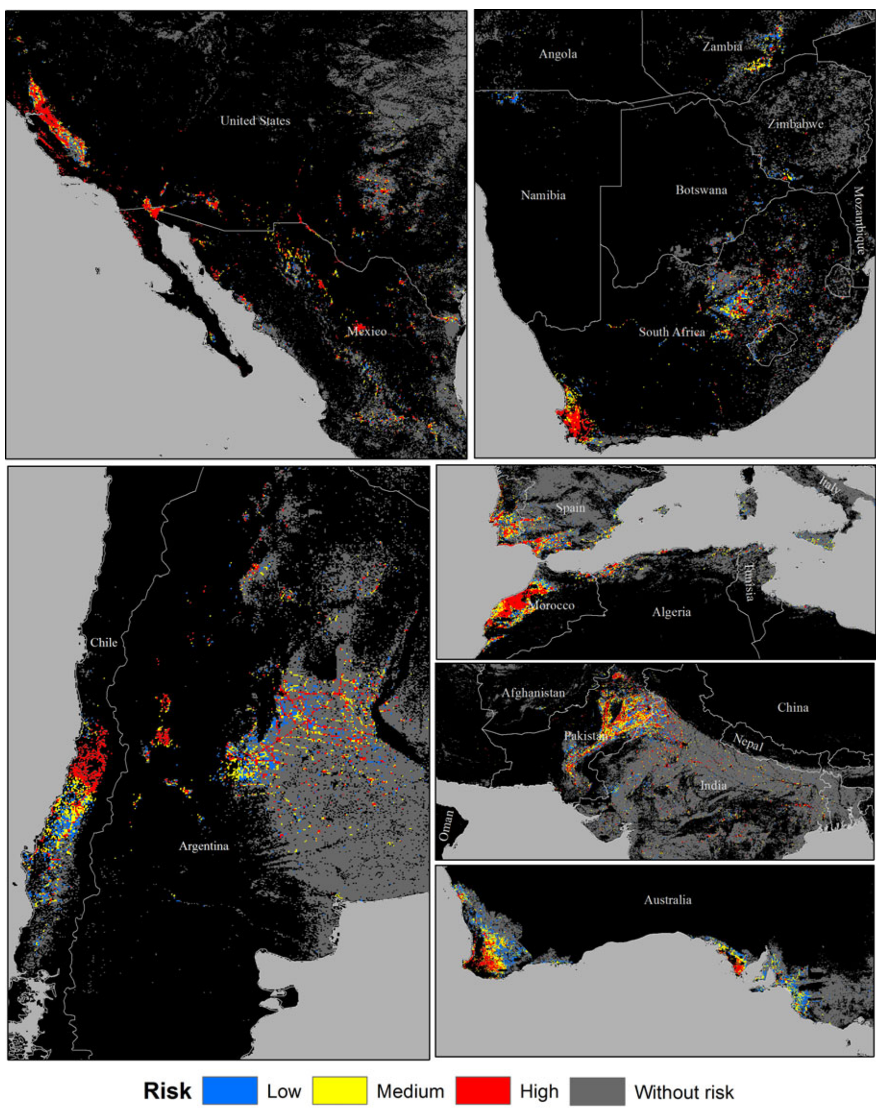

Figure 3. Distribution of potentially affected croplands by level of risk. Each map shows potentially affected zones. Cropland surfaces without risk estimated by the model are shown in gray (downloadable as File S2).

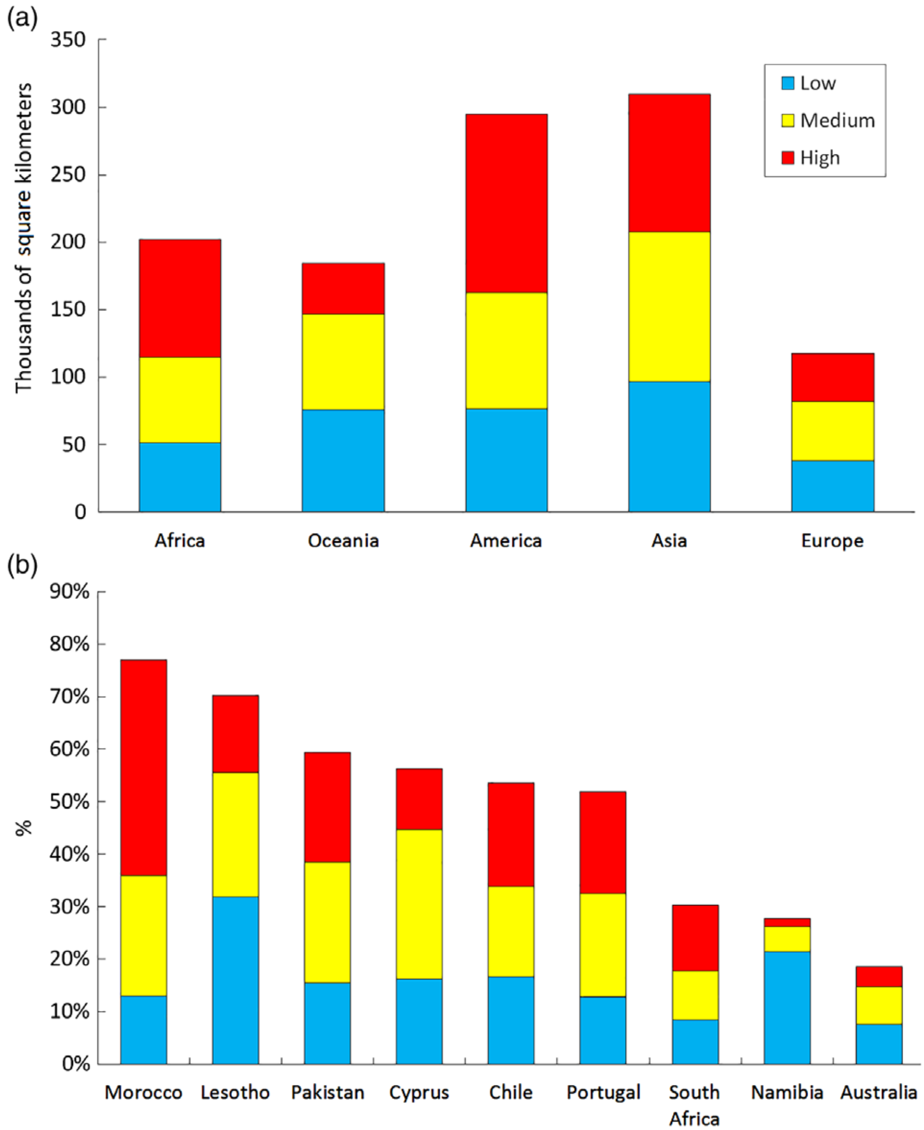

Figure 4. (a) Cropland area potentially affected by *Bagrada hilaris* per continent and level of risk. (b) Percentage of croplands potentially affected by *B. hilaris* in relation to the total cropland surface per country (downloadable as Files S3 and S4).

In America, 294 600 km^2 are potentially at risk; and 44.8% of the potentially affected croplands are at high level of risk. In Europe, 117 606.3 km^2 are at risk; 30.4% at a high level. In Africa, 229 007.3 km^2 are at risk; 43% at a high level. Oceania has 184 310.1 km^2 potentially affected by *B. hilaris*, equivalent to 16.2% of the total cropland within the continent. Of these potentially affected areas, 20.5% are at a high level of risk. In Asia, 309 659.8 km^2 are potentially affected, with 33% at a high level of risk (Figs 3 and 4a).

This pest could potentially be present in croplands of 54 countries worldwide, with 16 countries having > 10% of their total croplands potentially affected. The most affected countries by percentage of cropland areas potentially affected by *B. hilaris* are: Morocco (76.9%), Pakistan (59.4%), Chile (53.6%), Portugal (51.9%), Cyprus (31.3%), South Africa (30.3%), Namibia (27.4%), Lesotho (26.1%) and Australia (19.4%) (Fig. 4b).

In the case of the two selected zones, a predominance of high levels of risk was identified, followed by medium levels. In central Chile, the risk zone is located in the central valley from 32° to 37°S, with a total area of 5635.8 km^2 representing 80.8% of the susceptible crops. The risk levels are 50% high, 19.7% medium and 11.1% low. In California, the risk zone is located between 34° and 40°N, with a total area of 5779.7 km^2 which represents 70.9% of the susceptible crops. The risk levels are 43.7% high, 16.2% medium and 11% low (Fig. 5).

3.3 Estimation of future potential distribution of *B. hilaris* worldwide

Worldwide there is a change of 18.2% and 8.6% for the RCP scenarios 4.5 and 8.5, respectively. In North America, mainly the USA, the potential distribution range of *B. hilaris* will expand to higher latitudes similarly under both climate change scenarios, with the affected area changing by 24.4% and 21.3% in RCP 4.5 and 8.5, respectively (Fig. 6). In South Africa, the potential distribution under the RCP 4.5 climate change scenario would have a negative change in area (5.9%), expanding the potential distribution in Zimbabwe but contracting in South Africa, Botswana and

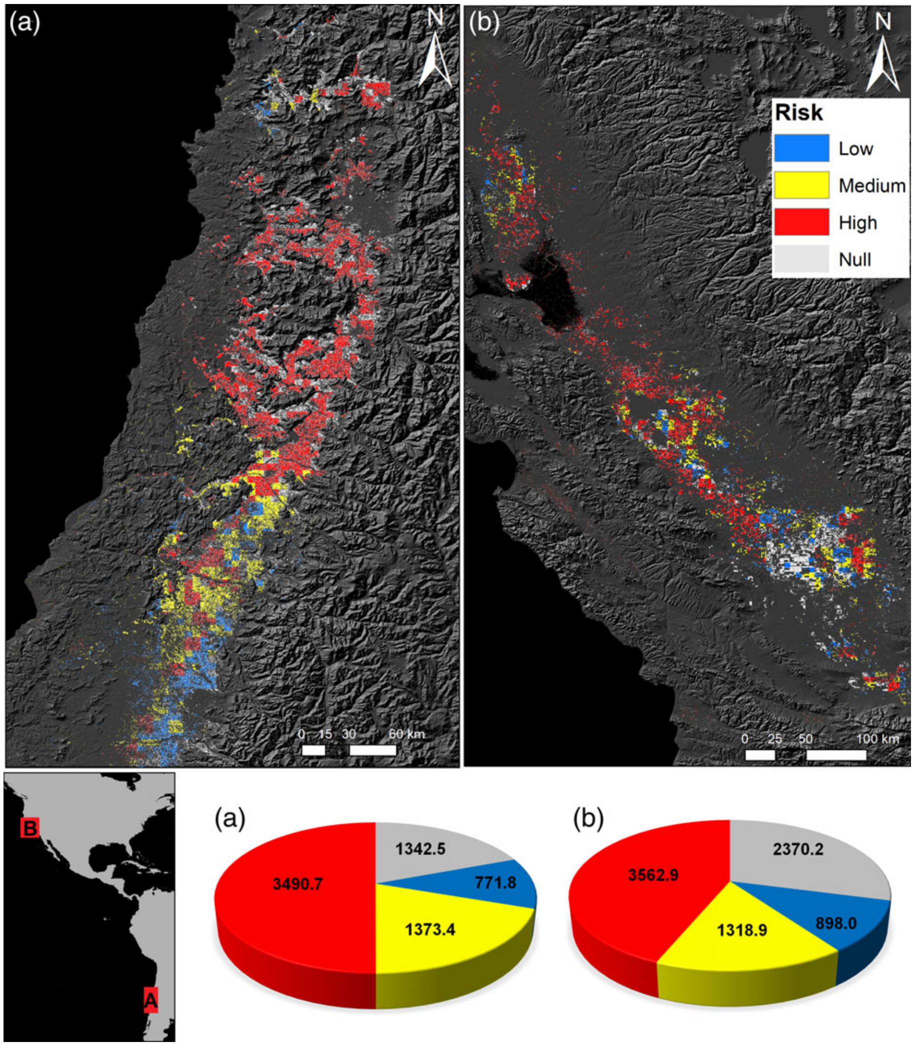

Figure 5. Potentially affected croplands in (a) Central Chile and (b) California, USA. (Upper) Spatial pattern of potentially affected croplands per level of risk. (Lower) Area potentially affected per level of risk expressed in km^2.

Namibia. By contrast, in South Africa the RCP 8.5 climate change scenario predicts an 18.1% change in the distribution range, mainly in the northern zone of the potential current distribution (Fig. 6). In South America, the potential distribution range of *B. hilaris* increases to the south of the current potential distribution, presenting a change of 108%, mainly in Argentina and Chile, with a significant increase in Patagonia. There is no significant difference between RCP 4.5 and 8.5 in terms of the overall shift in distribution range in South America, however in Chile, RCP 8.5 increases the potential distribution of *B. hilaris* by 37.3% more than RCP 4.5 (285 299.8 km^2 *vs*. 211 812.3 km^2 for RCP 8.5 and 4.5, respectively) (Fig. 6). In Asia, both climate change scenarios result in a contraction in the potential distribution range of *B. hilaris*, with changes of −42.3% and −62.3% for RCP 4.5 and 8.5, respectively (Fig. 7). In Australia, there are changes of 46.1% and 21.6% for RCP 4.5 and 8.5, respectively. In Europe, climate change results in mainly a contraction in the potential distribution, of −36.9% and −68.6% for RCP 4.5 and 8.5, respectively. In northern Africa, there is a preponderance of contraction in the potential distribution range, mainly in Morocco, Algeria and Tunisia, of −67.6% and −46% for RCP 4.5 and 8.5, respectively (Fig. 7). Climate change scenarios predict that *B. hilaris* could find suitable bioclimatic conditions in Colombia, Egypt, Niger and Venezuela (where it is not currently present), whereas Kazakhstan, Nepal, Turkmenistan, Malawi, Zimbabwe, Botswana and Chile the current suitable area is predicted to more than double under climate change scenarios.

4 DISCUSSION

4.1 Potentialities and assumptions

The predicted suitability of our model must be interpreted cautiously; in zones already colonized by *B. hilaris* the model represents the potential distribution of the pest in North America, Asia, Africa and Europe; whereas in zones where the species is not currently present it represents the potentially colonizable area, such as Oceania and South America (considering the recent arrival of the species).[38,41] The map of potential current distribution includes more specific information associated with the human footprint, whereas future scenarios are based only on climate projections plus topography. Considering that the human footprint was identified as the most important variable in the current model, not including it in future scenarios may affect the specificity of predictions. However, considering the high dispersal ability of invasive

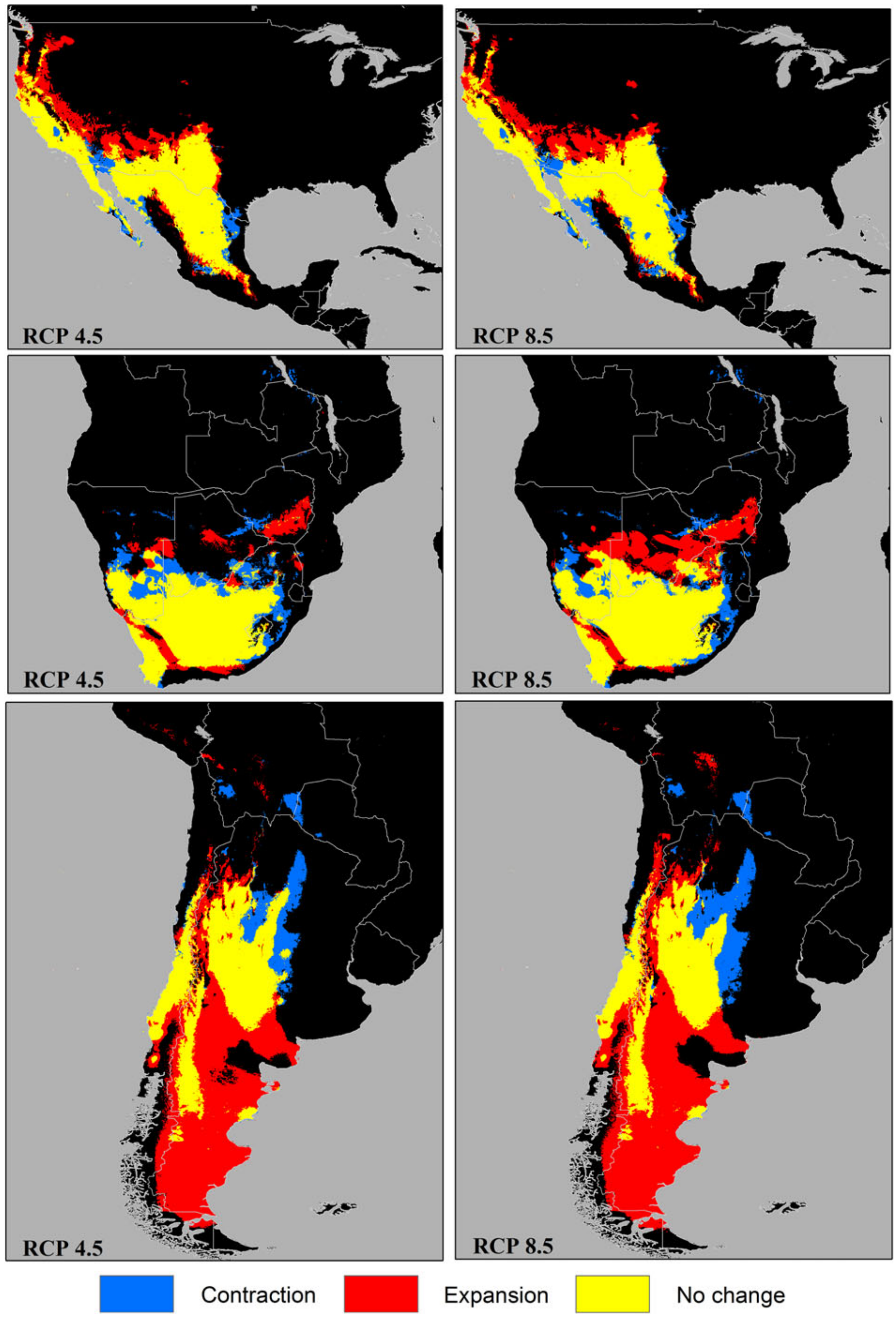

Figure 6. Shifts in potential distribution range of *Bagrada hilaris* under climate change scenarios in North America (upper), South Africa (middle) and southern South America (lower).

species, which usually have no dispersal restrictions,[65] we decided not to restrict the future distribution models by dispersion. The actual areas occupied will depend on the capacity of the organism to disperse across the new suitable zones, accessing these new available resources.[66,67] Nevertheless, our approach constitutes a baseline for estimation of the potential future spread and spatial distribution of *B. hilaris* under different climate change scenarios.

It is important to mention that occurrence of this pest and its success in the colonized zones depends on many other factors that are difficult to integrate into the model. Our approach allows an estimate of suitability based mainly on abiotic variables, which may be a proxy for abiotic resistance.[62] However, other factors related to the biotic characteristics of the colonized zones could influence pest failure or success, based on the biotic resistance hypothesis.[68] Factors such as the presence of predators and competitors might regulate *B. hilaris* growth rate associated with the control by natural enemies (predators, parasitoids) or through competitive exclusion (competitors).[68,69] Highly biodiverse communities increase the probability of biological control and functional redundancy by local species through the presence of predators and competitors that deal with the pest.[68,69] In addition, landscape configuration is essential for the regulation of invasive species, by modulating the spread and growth of the population, which depend on landscape structural and compositional traits.[70,71] Highly compositional and

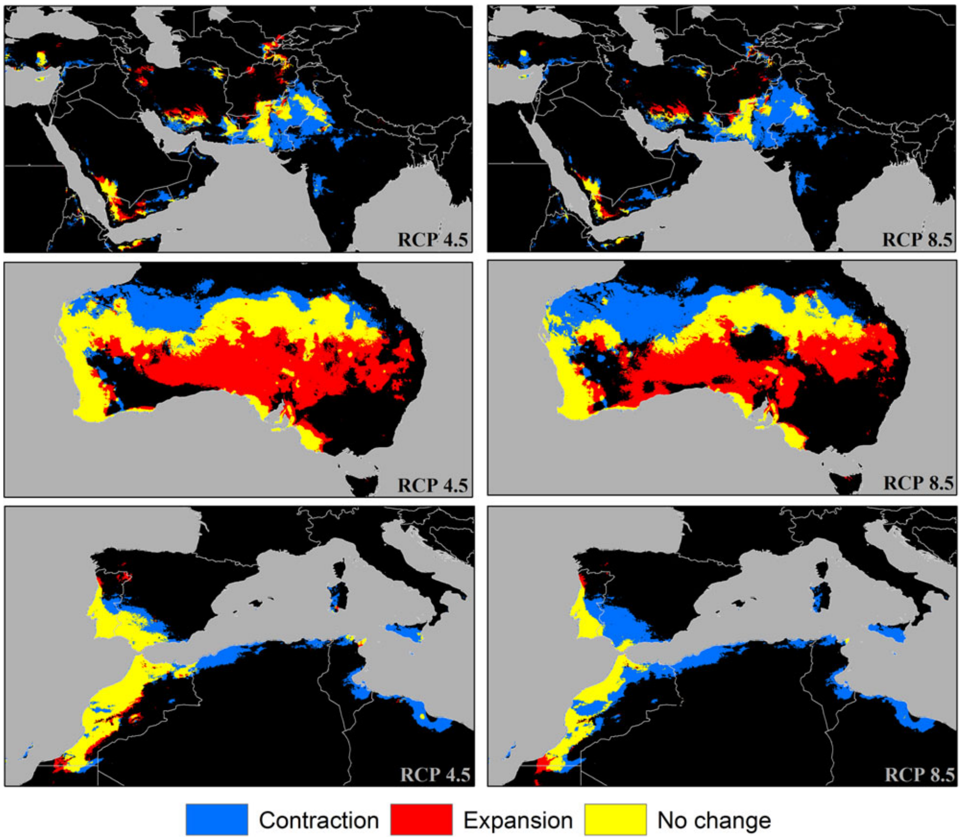

Figure 7. Shifts in potential distribution range of *Bagrada hilaris* under climate change scenarios in middle Asia (upper), Australia (middle) and Europe–North Africa (lower).

structural landscape heterogeneity influences the success of an invasive species, by increasing the availability of habitat types for other species (predators and competitors) and hindering the dispersion capacity of the invasive species across the landscape.[70–72] Hence, we recommend that agroecosystems management is focused on maximizing the ecological diversity of communities and landscape heterogeneity in zones that are or will be potentially affected by *B. hilaris*. Organic and traditional agricultural management strategies and cropland rotation regimes could benefit from the presence of natural enemies–competitors and landscape heterogeneity, allowing ecological control of the pest.[73]

4.2 *Bagrada hilaris* as a potential world threat

Our results show that *B. hilaris* has high environmental suitability in zones with Mediterranean and arid climates which have median isothermality with a scarcity of precipitation in the warmest quarter.[24] This species is unable to colonize zones with tropical or temperate climates, and is restricted to coastal zones at latitudes between 15° and 40° in both hemispheres (Fig. 2). Our model predicts that the 'human footprint' variable is a significant predictor of *B. hilaris* suitability with 47.8% contribution to the ENM. The species shows highly synanthropic behavior, increasing their suitability with human influence and disturbance. This could be associated with ecological traits in the species such as generalism, high tolerance and dispersal capacity, and be influenced by human factors such as globalization (increase in global trade), expansion of cropland limits, shifts to industrial agriculture and landscape homogenization.[13,71,74]

The geographic distribution of this species represents a serious threat to Mediterranean and arid zones, because water scarcity in these regions could make croplands highly vulnerable to the effects of *B. hilaris*, intensifying economic losses and threatening food security.[75,76] Control actions for this pest imply high economic investments, which may not be affordable for developing and poor countries and small-scale farmers who have limited resilience and adaptive capacity to deal with the magnitude of this pest.[18,77]

Another factor shown here is related to climate change, which modifies the future potential geographic distribution of *B. hilaris* worldwide, allowing colonization of new zones in some continents such as America and Australia. In other continents, climate change might contribute to abiotic control of this pest by decreasing the suitability of particular zones for this species (Figs 6 and 7). Nevertheless, in countries affected by drought and water scarcity, climate change will affect irrigated agriculture systems, limiting access to water for crop irrigation and intensifying the frequency and intensity of drought events.[10,12] These extreme events and the effect of *B. hilaris* could increase the economic losses associated with a decrease in the cropland success, the cost of pesticides and the accessibility to water resources for crop irrigation. Given the ectothermal physiology of this pest, studies have proposed that an increase in temperature in Mediterranean and Temperate zones could induce an increase in the growth rate and activity of phytophagous insects, leading to the need to use huge amounts of pesticides to maintain productivity.[78] Considering that *B. hilaris* presents a seasonal crop distribution and different plant hosts during the year, climate change could generate shifts in these seasonal and phenological patterns, forcing changes in seasonal management strategies.[13,18] These effects could imply changes in organic and traditional farming practices, forcing the use of pesticides, incurring in new costs and affecting the target markets of producers.[77]

The results presented here highlight *B. hilaris* as a global problem, with a potentially affected cropland area equivalent to the surface area of South Africa and presenting suitability in all continents. We generated a series of maps that provide guidance on the spatial dimension of the *B. hilaris* threat, identifying its global distribution, cropland areas potentially affected and their levels of risk. These maps may be useful to practitioners in the prevention, management and control of *B. hilaris*, constituting a spatially explicit tool to deal with this threat. The projections shown here point out potential zones of expansion and contraction in the distribution of *B. hilaris*. Considering the global scale of our analysis, the results constitute a baseline for governments to develop more detailed national or regional assessment of this pest.

ACKNOWLEDGEMENTS

We appreciate the help of Dr Cecilia Hidalgo of the Universidad de Chile in the revision and correction of the English language and grammar of this study.

SUPPORTING INFORMATION

Supporting information may be found in the online version of this article.

REFERENCES

1 Pimentel D, McNair S, Janecka J, Wightman J, Simmonds C, O'Connell C *et al.*, Economic and environmental threats of alien plant, animal, and microbe invasions. *Agric Ecosyst Environ* **84**:1–20 (2001).
2 Butchart SHM, Walpole M, Collen B, van Strien A, Scharlemann JPW, Almond REA *et al.*, Global biodiversity: indicators of recent declines. *Science* **328**:1164 LP–1168 (2010).
3 Parsa S, Kondo T and Winotai A, The cassava mealybug (*Phenacoccus manihoti*) in Asia: first records, potential distribution, and an identification key. *PLoS One* **7**:e47675 (2012).
4 Harwood JD and Parajulee MN, Global impact of biological invasions: transformation in pest management approaches. *Biol Invasions* **12**:2855–2856 (2010).
5 Hulme PE, Climate change and biological invasions: evidence, expectations, and response options. *Biol Rev* **92**:1297–1313 (2017).
6 Oliveira CM, Auad AM, Mendes SM and Frizzas MR, Economic impact of exotic insect pests in Brazilian agriculture. *J Appl Entomol* **137**:1–15 (2013).
7 Hulme PE, Trade, transport and trouble: managing invasive species pathways in an era of globalization. *J Appl Ecol* **46**:10–18 (2009).
8 Bebber DP, Range-expanding pests and pathogens in a warming world. *Annu Rev Phytopathol* **53**:335–356 (2015).
9 Andrew NR and Hill SJ, Effect of climate change on insect pest management, in *Environmental Pest Management*: Challenges for Agronomists, Ecologists, Economists and Policymakers, ed. by Call M. Wiley, INRA, Sophia Antipolis, France. pp. 195–223 (2017).
10 Gornall J, Betts R, Burke E, Clark R, Camp J, Willett K *et al.*, Implications of climate change for agricultural productivity in the early twenty-first century. *Philos Trans R Soc, B* **365**:2973–2989 (2010).
11 Wheeler T and Von Braun J, Climate change impacts on global food security. *Science* **288**:285–288 (2013).
12 Campbell BM, Vermeulen SJ, Aggarwal PK, Corner-dolloff C, Girvetz E, Maria A *et al.*, Reducing risks to food security from climate change. *Global Food Secur* **11**:34–43 (2016).
13 Palumbo JC, Perring TM, Millar JG and Reed DA, Biology, ecology, and management of an invasive stink bug, *Bagrada hilaris*, in North America. *Annu Rev Entomol* **61**:453–473 (2016).
14 Reed DA, Palumbo JC, Perring TM and May C, *Bagrada hilaris* (Hemiptera: Pentatomidae), an invasive stink bug attacking cole crops in the Southwestern United States. *J Integr Pest Manag* **4**:C1–C7 (2013).
15 Huang TI, Reed DA, Perring TM and Palumbo JC, Feeding damage by *Bagrada hilaris* (Hemiptera: Pentatomidae) and impact on growth and chlorophyll content of Brassicaceous plant species. *Arthropod Plant Interact* **8**:89–100 (2014).
16 Palumbo JC and Carrière Y, Association between *Bagrada hilaris* density and feeding damage in broccoli: implications for pest management. *Plant Health Prog* **16**:158–162 (2015).
17 Palumbo JC and Natwick ET, The *Bagrada* bug (Hemiptera: Pentatomidae): a new invasive pest of cole crops in Arizona and California. *Plant Health Prog* **49**:2–4 (2010).
18 Palumbo JC, Impact of *Bagrada* bug infestations on desert cole crops from 2010–2014 (May 13, 2015), in *Vegetable IPM update archives*. Univ. Arizona, Coop. Ext., Tucson, Vol. **6**, No. 10. (2015) http://ag.arizona.edu/crops/vegetables/advisories/more/insect132.html.
19 Joseph SV, Grettenberger I and Godfrey L, Insecticides applied to soil of transplant plugs for *Bagrada hilaris* (Burmeister) (Hemiptera: Pentatomidae) management in broccoli. *Crop Prot* **87**:68–77 (2016).
20 Faúndez EI, Lüer A, Rider D, Faúndez EI, Lüer A, Cuevas ÁG *et al.*, First record of the painted bug *Bagrada hilaris* (Burmeister, 1835) (Heteroptera: Pentatomidae) in South America. *Arquivos Entomoloxicos* **16**:175–179 (2016).
21 Faúndez EI, Lüer A and Cuevas A, The establishment of *Bagrada hilaris* (Burmeister, 1835) (Heteroptera: Pentatomidae) in Chile, an avoidable situation? *Arquivos Entomolóxicos* **17**:239–241 (2017).
22 SAG, Resolución exenta No. 1577/2017. Servicio Agricola Ganadero, Ministerio de Agricultura de Chile. p. 4. (2017) http://www.sag.gob.cl/sites/default/files/res_1577-2017._co_b._hilaris_17.03.17.pdf.
23 Phillips SJ, Anderson RP, Dudík M, Schapire RE and Blair ME, Opening the black box: an open-source release of Maxent. *Ecography (Cop)* **40**:887–893 (2017).
24 Fick SE and Hijmans RJ, WorldClim 2: new 1-km spatial resolution climate surfaces for global land areas. *Int J Climatol* **37**:4302–4315 (2017).
25 Sedac – N.A.S.A. Wildlife Conservation Society – WCS and Center for International Earth Science Information Network – CIESIN – Columbia University, Last of the Wild Project, Version 2, 2005 (LWP-2): Global Human Footprint Dataset (Geographic). Palisades, NY: NASA Socioeconomic Data and Applications Center (SEDAC) (2005).
26 GBIF.org (22 August 2017) GBIF Occurrence Download https://doi.org/10.15468/dl.nbtw1v (2017)
27 Chacko MJ and Katiyar RN, *Hadrophanurus karnalensis* sp. n. (hymenoptera: scelionidae), a parasite of *Bagrada cruciferarum* kirkaldy (Hemiptera: Pentatomidae). *Proc R Entomol Soc Lond Ser B Gen Entomol* **30**:161–163 (1961).
28 Saljoqi AUR, Sadur-Rehman HN and Khan SA, Insect pests of canola crop (other than aphid). *J Agric Biol Sci* **1**:19–21 (2006).
29 De Pasquale C, Guarino S, Peri E, Alonzo G and Colazza S, Investigation of cuticular hydrocarbons from *Bagrada hilaris* genders by SPME/GC-MS. *Anal Bioanal Chem* **389**:1259–1265 (2007).
30 Ahuja B, Kalyan RK, Ahuja UR, Singh SK, Sundria MM and Dhandapani A, Integrated management strategy for painted bug, *Bagrada hilaris* (Burm) inflicting injury at seedling stage of mustard (*Brassica juncea*) in arid western Rajasthan. *Pestic Res J* **20**:48–51 (2008).
31 Bundy CS, Grasswitz TR and Sutherland C, First report of the invasive stink bug *Bagrada hilaris* (Burmeister) (Heteroptera: Pentatomidae) from New Mexico, with notes on its biology. *Southwest Entomol* **37**:411–414 (2012).
32 Sanchez-Pena SR, First record in Mexico of the invasive stink bug *Bagrada hilaris*, on cultivated crucifers in Saltillo. *Southwest Entomol* **39**:375–377 (2014).
33 Mahmood R, Jones WA, Bajwa BE and Rashid K, Egg parasitoids from Pakistan as possible classical biological control agents of the invasive pest *Bagrada hilaris* (Heteroptera: Pentatomidae). *J Entomol Sci* **50**:147–149 (2015).
34 Torres-Acosta RI and Sánchez-Peña SR, Geographical distribution of *Bagrada hilaris* (Hemiptera: Pentatomidae) in Mexico. *Ga. Entomol. Soc* **51**:165–167 (2016).
35 Brown JL, SDMtoolbox: a python-based GIS toolkit for landscape genetic, biogeographic and species distribution model analyses. *Methods Ecol Evol* **5**:694–700 (2014).
36 Royston PA, Simple method for evaluating the Shapiro–Francia W' test of non-normality. *Stat* **32**:297–300 (1983).

37 Bradley C, The absolute correlation coefficient. *Math Gaz* **69**:12–17 (1985).
38 Elith J and Leathwick J, Species distribution models: ecological explanation and prediction across space and time. *Annu Rev Ecol Evol Syst* **40**:677–697 (2009).
39 Elith J, Phillips SJ, Hastie T, Dudík M, Chee YE and Yates CJ, A statistical explanation of MaxEnt for ecologists. *Divers Distrib* **17**:43–57 (2011).
40 Gallien L, Douzet R, Pratte S, Zimmermann NE and Thuiller W, Invasive species distribution models – how violating the equilibrium assumption can create new insights. *Glob Ecol Biogeogr* **21**:1126–1136 (2012).
41 Hill MP, Gallardo B and Terblanche JS, A global assessment of climatic niche shifts and human influence in insect invasions. *Glob Ecol Biogeogr* **26**:679–689 (2017).
42 Congalton RG, Yadav K, McDonnell K et al, NASA Making Earth System Data Records for Use in Research Environments (MEaSUREs) Global Food Security-support Analysis Data (GFSAD) @ 30-m: Cropland Extent Validation (GFSAD30VAL). NASA EOSDIS Land Processes DAAC (2017). Retrieved from https://doi.org/10.5067/MEaSUREs/GFSAD/GFSAD30VAL.001
43 Zhong, Y., Giri, C., Thenkabail, P.S., Teluguntla, P., Congalton, R. G., Yadav, K. et al. NASA Making Earth System Data Records for Use in Research Environments (MEaSUREs) Global Food Security-support Analysis Data (GFSAD) @ 30-m for South America: Cropland Extent Product (GFSAD30SACE). NASA EOSDIS Land Processes DAAC (2017). Retrieved from https://doi.org/10.5067/MEaSUREs/GFSAD/GFSAD30SACE.001
44 Massey R, Sankey TT, Yadav K, Congalton RG, Tilton JC, Thenkabail PS NASA Making Earth System Data Records for Use in Research Environments (MEaSUREs) Global Food Security-support Analysis Data (GFSAD) @ 30m for North America: Cropland Extent Product (GFSAD30NACE). NASA EOSDIS Land Processes DAAC (2017). https://doi.org/10.5067/MEaSUREs/GFSAD/GFSAD30NACE.001
45 Phalke A, Ozdogan M, Thenkabail S, et al. NASA Making Earth System Data Records for Use in Research Environments (MEaSUREs) Global Food Security-support Analysis Data (GFSAD) @ 30-m for Europe, Middle-east, Russia and Central Asia: Cropland Extent Product (GFSAD30EUCEARUMECE). NASA EOSDIS Land Processes DAAC (2017). Retrieved from https://doi.org/10.5067/MEaSUREs/GFSAD/GFSAD30EUCEARUMECE.001
46 Gumma MK, Thenkabail PS, Teluguntla PG, Rao MN, Mohammed IA and Whitbread AM, Mapping rice–fallow cropland areas for short-season grain legumes intensification in South Asia using MODIS 250 m time-series data. *Int J Digit Earth* **9**:981–1003 (2016).
47 Oliphant AJ, Thenkabail PS, Teluguntla P, et al, NASA Making Earth System Data Records for Use in Research Environments (MEaSUREs) Global Food Security-support Analysis Data (GFSAD) @ 30-m for Southeast & Northeast Asia: Cropland Extent Product (GFSAD30SEACE). NASA EOSDIS Land Processes DAAC (2017). Retrieved from https://doi.org/10.5067/MEaSUREs/GFSAD/GFSAD30SEACE.001
48 Teluguntla P, Thenkabail PS, Xiong J, Gumma MK, Congalton RG, Oliphant A *et al.*, Spectral matching techniques (SMTs) and automated cropland classification algorithms (ACCAs) for mapping croplands of Australia using MODIS 250-m time-series (2000–2015) data. *Int J Digit Earth* **10**:944–977, Taylor & Francis (2017).
49 Teluguntla P, Thenkabail PS, Xiong J, et al, NASA Making Earth System Data Records for Use in Research Environments (MEaSUREs) Global Food Security-support Analysis Data (GFSAD) @ 30-m for Australia, New Zealand, China, and Mongolia: Cropland Extent Product (GFSAD30AUNZCNMOCE). NASA EOSDIS Land Processes DAAC (2017). Retrieved from https://doi.org/10.5067/MEaSUREs/GFSAD/GFSAD30AUNZCNMOCE.001
50 Xiong J, Thenkabail PS, Tilton JC, et al. NASA Making Earth System Data Records for Use in Research Environments (MEaSUREs) Global Food Security-support Analysis Data (GFSAD) @ 30-m Africa: Cropland Extent Product (GFSAD30AFCE). NASA EOSDIS Land Processes DAAC (2017). Retrieved from https://doi.org/10.5067/MEaSUREs/GFSAD/GFSAD30AFCE.001
51 Xiong J, Thenkabail PS, Gumma MK, Teluguntla P, Poehnelt J, Congalton RG *et al.*, Automated cropland mapping of continental Africa using Google Earth engine cloud computing. *ISPRS J Photogramm Remote Sens* **126**:225–244 (2017).
52 Xiong J, Thenkabail PS, Tilton JC, Gumma MK, Teluguntla P, Oliphant A *et al.*, Nominal 30-m cropland extent map of continental Africa by integrating pixel-based and object-based algorithms using Sentinel-2 and Landsat-8 data on Google earth engine. *Remote Sens* **9**:1065 (2017).
53 USDA National Agricultural Statistics Service Cropland Data Layer. Published crop-specific data layer [Online]. Available at https://nassgeodata.gmu.edu/CropScape/ (accessed {DATE}; verified {DATE}). USDA-NASS, Washington, DC (2017).
54 Hill D, *Agricultural Insect Pests of the Tropics and their Control*, 1st edn. Cambridge University Press, Cambridge, UK (1975).
55 Gupta JC and Gupta DS, Note on some new hosts of the painted-bug (*Bagrada cruciferarum* Kirk.: Pentatomidae, Heteroptera). *Indian J Agric Sci* **40**:645–646 (1970).
56 Joseph SV, Grettenberger I, Godfrey L and Zavala N, Susceptibility of germinating cruciferous seeds to *Bagrada hilaris* (Hemiptera: Pentatomidae) feeding injury. *Arthropod Plant Interact* **11**:577–590 (2017).
57 Zhao Y, Feng D, Yu L, Wang X, Chen Y, Bai Y *et al.*, Detailed dynamic land cover mapping of Chile: accuracy improvement by integrating multi-temporal data. *Remote Sens Environ* **183**:170–185 (2016).
58 Bellard C, Bertelsmeier C, Leadley P, Thuiller W and Courchamp F, Impacts of climate change on the future of biodiversity. *Ecol Lett* **15**:365–377 (2012).
59 Ashraf U, Peterson AT, Chaudhry MN, Ashraf I, Saqib Z, Rashid Ahmad S *et al.*, Ecological niche model comparison under different climate scenarios: a case study of Olea spp. in Asia. *Ecosphere* **8**:e01825–n/a (2017).
60 Hodd RL, Bourke D and Skeffington MS, Projected range contractions of European protected oceanic montane plant communities: focus on climate change impacts is essential for their future conservation. *PLoS One* **9**:e95147 (2014).
61 Intergovernmental Panel for Climate Change, *Fifth Assessment Report*. Cambridge University Press, Cambridge (2014).
62 Bi D, Dix M, Marsland SJ, O'Farrell S, Rashid H, Uotila P *et al.*, The ACCESS coupled model: description, control climate and evaluation. *Aust Meteorol Ocean J* **63**:41–64 (2013).
63 Watanabe M, Suzuki T, O'ishi R *et al.*, Improved climate simulation by MIROC5: mean states, variability, and climate sensitivity. *J Climate* **23**:6312–6335 (2010).
64 Kay JE, Deser C, Phillips A, Mai A, Hannay C, Strand G *et al.*, The community earth system model (CESM) large ensemble project: a community resource for studying climate change in the presence of internal climate variability. *Bull Am Meteorol Soc* **96**:1333–1349 (2015).
65 Mestre A, Aguilar-Alberola JA, Baldry D, Balkis H, Ellis A, Gil-Delgado JA *et al.*, Invasion biology in non-free-living species: interactions between abiotic (climatic) and biotic (host availability) factors in geographical space in crayfish commensals (Ostracoda, Entocytheridae). *Ecol Evol* **3**:5237–5253 (2013).
66 Soberon J and Nakamura M, Niches and distributional areas: concepts, methods, and assumptions. *Proc Natl Acad Sci U S A* **106**:19644–19650 (2009).
67 Nuñez MA and Medley KA, Pine invasions: climate predicts invasion success; something else predicts failure. *Divers Distrib* **17**:703–713 (2011).
68 Perkins LB, Leger EA and Nowak RS, Invasion triangle: an organizational framework for species invasion. *Ecol Evol* **4**:610–625 (2011).
69 Zenni RD and Nuñez MA, The elephant in the room: the role of failed invasions in understanding invasion biology. *Oikos* **122**:801–815 (2013).
70 O'Reilly-Nugent A, Palit R, Lopez-Aldana A, Medina-Romero M, Wandrag E and Duncan RP, Landscape effects on the spread of invasive species. *Curr Landscape Ecol Rep* **1**:107–114 (2016).
71 Gamez-Virues S, Perovic DJ, Gossner MM, Borschig C, Bluthgen N, de Jong H *et al.*, Landscape simplification filters species traits and drives biotic homogenization. *Nat Commun* **6**:8568 (2015).
72 Fraser EJ, Lambin X, Travis JM, Harrington LA, Palmer SC, Bocedi G *et al.*, Range expansion of an invasive species through a heterogeneous landscape – the case of American mink in Scotland. *Divers Distrib* **21**:888–900 (2015).
73 Winqvist C, Bengtsson J, Aavik T, Berendse F, Clement LW, Eggers S *et al.*, Mixed effects of organic farming and landscape complexity on farmland biodiversity and biological control potential across Europe. *J Appl Ecol* **48**:570–579 (2011).
74 Seebens H, Essl F, Dawson W, Fuentes N, Moser D, Pergl J *et al.*, Global trade will accelerate plant invasions in emerging economies under climate change. *Glob Change Biol* **21**:4128–4140 (2015).

75 De Wrachien D, Ragab R, Hamdy A and Trisorio Liuzzi G, Global warming water scarcity and food security in the Mediterranean environment. Options Méditerranéennes. Série A Séminaires Méditerranéens, in *Food Security Under Water Scarcity in the Middle East: Problems and Solutions*, ed. by Hamdy A and Monti R. CIHEAM, Bari, p. 444 (2005).
76 De Chattel F, Holst-Warhaft G and Steenhuis T eds, *Water Scarcity, Security and Democracy: a Mediterranean Mosaic*. Global Water Partnership Mediterranean, Cornell University and the Atkinson Center for a Sustainable Future, Ithaca, NY, p. 178 (2014).
77 Parsa S, Morse S, Bonifacio A, Chancellor TCB, Condori B, Crespo-Perez V *et al.*, Obstacles to integrated pest management adoption in developing countries. *Proc Natl Acad Sci* **111**:3889–3894 (2014).
78 Taylor R, Herms D, Cardina J and Moore R, Climate change and pest management: unanticipated consequences of trophic dislocation. *Agronomy* **8**:7 (2018).

